

# EFFECT OF LEO EXPOSURE ON AROMATIC POLYMERS CONTAINING PHENYLPHOSPHINE OXIDE GROUPS

K.A. Watson<sup>1</sup>, S. Ghose<sup>1</sup>, P.T. Lillehei<sup>2</sup>, J.G. Smith, Jr.<sup>2</sup>, and J.W. Connell<sup>2</sup>

<sup>1</sup>National Institute of Aerospace  
100 Exploration Way  
Hampton VA 23666

<sup>2</sup>National Aeronautics and Space Administration  
Langley Research Center  
Hampton VA 23681-2199

**Abstract** As part of the Materials on The International Space Station Experiment (MISSE), aromatic polymers containing phenylphosphine oxide groups were exposed to low Earth orbit for ~4 years. All of the aromatic polymers containing phenylphosphine oxide groups survived the exposure despite the high fluence of atomic oxygen that completely eroded other polymer films such as Kapton<sup>®</sup> and Mylar<sup>®</sup> of comparable or greater thickness. The samples were characterized for changes in physical properties, thermal/optical properties surface chemistry, and surface topography. The data from the polymer samples on MISSE were compared to samples from the same batch of material stored under ambient conditions on Earth. In addition, comparisons were made between the MISSE samples and those subjected to shorter term space flight exposures. The results of these analyses will be presented.

This paper is work of the U. S. Government and is not subject to copyright protection in the U.S.

**1. INTRODUCTION** Aromatic polymers containing phenylphosphine oxide (PPO) groups have been under investigation for over a decade [1-4]. Along with providing both solubility and high glass transition temperature (T<sub>g</sub>) without sacrificing mechanical properties, PPO groups were also shown to improve the resistance of the polymer to oxygen plasma and atomic oxygen (AO) by a self passivating effect in which a phosphate enriched surface layer is formed protecting the underlying material from further reaction [5-9]. Until now, there has been no data available regarding the long term (> 1 year) performance of these types of polymers in low Earth orbit (LEO).

The push to develop AO resistant polymers dates back to pre-space station days and since that time a variety of approaches have been investigated. Some of the early work involved polyphosphazenes [10,11]. In addition, a large variety of silicon (Si) containing polymers were investigated in which the Si was typically incorporated in the form of an organic species such as a siloxane unit [12-21]. In both cases, the formation of an oxide rich surface layer by the reaction of phosphorus (P) or Si with atomic oxygen was observed. This oxide surface layer reduced the subsequent reaction efficiency with AO and protected the underlying polymeric material. Other approaches involved highly

fluorinated polymers [13, 22-23], metal oxide coatings [23-25], and incorporating POSS molecules into polymers as a means of achieving AO resistance [26-28].

MISSE 1 and 2 consisted of two experiment carriers (PECs) of specimens that were attached to the International Space Station (ISS) and passively exposed to the LEO environment (including AO and ultraviolet radiation). The materials were deployed in August 2001 and retrieved in August 2005. One PEC was intended to experience exposure in the flight (RAM) direction and the other in the WAKE direction. However, due to the orbital configuration of the ISS, the WAKE exposed samples experienced more AO fluence than expected. The results of this space flight exposure, particularly of AO exposure, on select aromatic polymers containing PPO groups will be presented.

## 2. EXPERIMENTAL

**2.1 Materials** The polymers consisted of a colorless polyimide film and a poly(arylene ether benzimidazole) film and thread. The polyimide film was prepared at NASA Langley Research Center following a procedure previously reported [30]. The poly(arylene ether benzimidazole) film (TOR-LM) was metallized with a 100 nm thick coating of vapor deposited aluminum (VDA). The film (38  $\mu\text{m}$ , 1.5 mil thick) was mounted such that the polymer surface faced the RAM direction. Both the TOR-LM film [9] and thread (TOR) [6] were obtained from Triton Systems, Inc. in 2000.

**2.2 Flight Exposure Conditions [29]** The film samples were 10.2 cm x 10.2 cm (4 in x 4 in) and 25 to 40  $\mu\text{m}$  thick and were mounted on an aluminum plate and held in place with metal strips. The conditions experienced during exposure for this set of samples (RAM facing side) were as follows: AO fluence from 6.5 to 9.1 x 10<sup>21</sup> atoms/cm<sup>2</sup>; equivalent solar hours 5870 to 6134 depending on exact sample location; thermal cycling, minimum temperature ~ -55 °C, maximum temperature ~ 66 °C, average temperature -13 °C. The normal orbital period was ~90 minutes.

**2.3 Characterization** Fourier transform infrared (FTIR) spectroscopy was performed on a Nicolet Magna-IR 560 ESP spectrometer. The %T through thin films was measured at 500 nm using a Perkin-Elmer Lambda 900 UV/VIS/NIR spectrometer. Solar absorptivities ( $\alpha$ ) of thin films were measured on an AZTek Model LPSR-300 spectrophotometer with measurements taken between 250 to 2800 nm using a vapor deposited aluminum on Kapton<sup>®</sup> film (1<sup>st</sup> surface mirror) as a reflective reference per ASTM E903-82. An AZTek Temp 2000A infrared reflectometer was used to measure the thermal emissivity ( $\epsilon$ ) of thin films. X-ray photoelectron spectroscopy (XPS) was performed using a VG XPS system. For analysis, 1253 eV X-rays from a magnesium anode were used and photo-electron energies were resolved using a hemispherical energy analyzer. Atomic force microscopy (AFM) was performed using a Digital Instruments MultiMode Scanning Probe Microscope (Veeco Metrology, Inc.). The samples were imaged in TappingMode and analyzed for surface roughness. Both the average ( $R_a$ ) and the root mean square ( $R_q$ ) roughness were recorded at several locations per sample [31].

## 3. RESULTS AND DISCUSSION

**3.1 Materials** The chemical structures of the aromatic polymers containing PPO groups are presented in Figure 1 and consist of a colorless polyimide (CP) film, a polybenzimidazole (TOR-LM) film with one side coated with VDA, and a

polybenzimidazole thread (TOR). The polymer samples were mounted in the exposure tray as shown in Figure 2. Control films and threads were cut from the same batch of material as that used in the flight experiment. The control samples were maintained in zip-lock bags under ambient conditions until the return of the flight specimens.

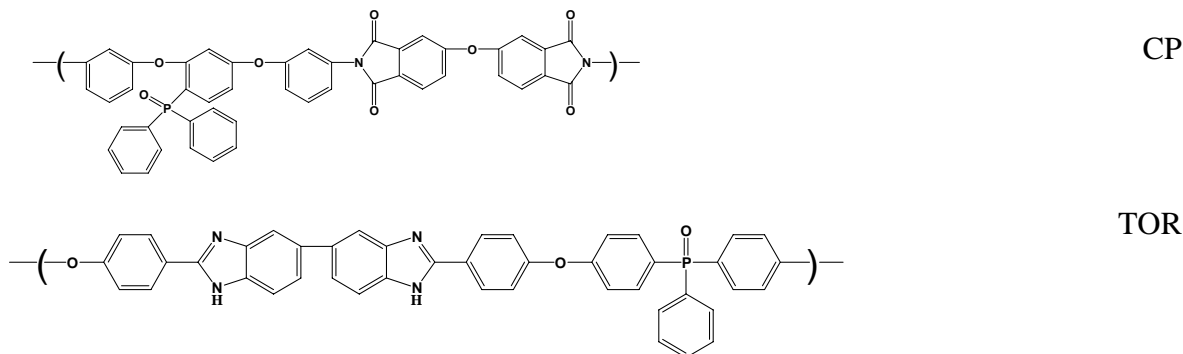


Figure 1. Chemical structure of polymer samples. TOR-LM is a 1:1 random copolymer of TOR (chemical structure above) with 4,4'-biphenol.

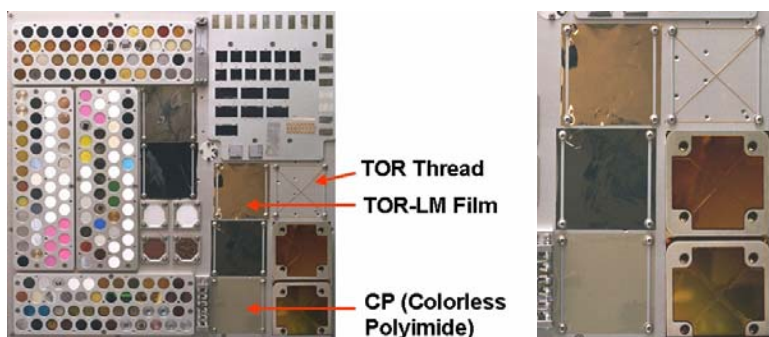


Figure 2. Samples mounted on exposure tray. A close-up is shown on the right.

**3.2 Flight Exposure Conditions** It is important to recognize that the flight samples were exposed to LEO where there is no molecular oxygen or water vapor. When returned to Earth for analysis, the samples were exposed to the ambient atmosphere, thus the potential exists for the surface chemistry to have been affected by this exposure.

Throughout the 4-year exposure, many samples did not survive the high AO fluence. For example, relatively thick (127  $\mu\text{m}$ ) Kapton<sup>®</sup> HN samples were completely eroded. Other polymer films such as Mylar<sup>®</sup>, metallized polyimides, and polybenzoxazole were also completely eroded. The flight samples were exposed to an AO fluence of 6.5 to 9.1  $\times 10^{21}$  atoms/cm<sup>2</sup> with simultaneous exposure to thermal cycling and UV and particulate radiation.

Aromatic polymers containing PPO groups have previously been exposed to both simulated AO as well as AO in short term space flight exposure experiments. From these experiments a few general conclusions were derived. Upon exposure to AO aromatic polymers containing PPO groups generally exhibit a two stage erosion process. In the first stage material is lost via the reaction of AO with the polymer to form small organic molecules that are subsequently lost via volatilization, simultaneously the AO exposed surface becomes enriched with a phosphate layer, eventually forming a polyphosphate surface layer. In the second stage AO erosion is significantly lessened due to the reduced

reactivity between the polyphosphate layer and AO. Evidence for this comes from the erosion rate, XPS,  $^{31}\text{P}$  nuclear magnetic resonance (NMR) spectroscopy, and X-ray adsorption near edge spectroscopy (XANES) analyses [2-8, 32]. In prior space flight exposure experiments involving aromatic polymers containing PPO groups the samples were exposed to AO fluences of  $7 \times 10^{19}$  atoms/cm<sup>2</sup> [5, 7] and  $1 \times 10^{19}$  atoms/cm<sup>2</sup> [8]. Based on these results, it was determined that aromatic polymers containing PPO groups had a reaction efficiency of about 15 times less than that of Kapton<sup>®</sup> HN.

**3.3 Visual Inspection of Flight Specimens** Samples were returned to NASA Langley Research Center in October 2005 and placed in a clean room for observation and subsequent deintegration. Pictures of the returned specimens still mounted in the PEC are presented in Figure 3. Both film samples had cracks adjacent to the metal bars and near the bolt holding the sample against the plate. A closeup of the TOR-LM film at a corner is also shown in Figure 3. The cracks are likely due to stress build-up as a result of the thermal expansion mismatch between the metal bars and the polymer. Both the TOR-LM and CP film samples appeared diffuse as a result of AO erosion and the CP film was no longer transparent. There was no visible erosion or obvious deterioration of the thread sample. The samples were subsequently removed from the PEC for additional characterization. The films were not brittle or fragile and did not suffer further deterioration upon handling and manipulation. Both films exhibited sufficient toughness such that they could be creased without visible damage, cracking, or fracture. In comparing these visual results with those from previous flight experiments [5,7,8], the previous samples were not visibly frosted and remained transparent, however the AO fluence was only in the range of  $1\text{-}7 \times 10^{19}$  atoms/cm<sup>2</sup>.

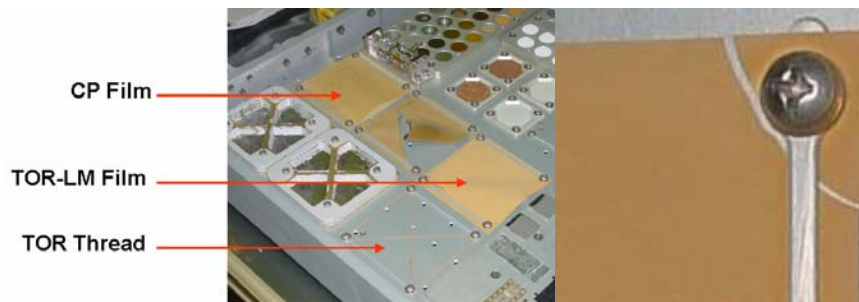


*Figure 3. Samples after return from LEO (left) and a close-up of TOR-LM (right) showing a crack in the film.*

**3.4. Characterization** FTIR was performed on the CP and TOR-LM films. In the CP film, the carbonyl peaks readily visible in the spectra corresponding to the control sample are significantly dampened in the spectra of the exposed film. This was the general trend for the bulk of the other significant FTIR spectral features as well as for the control and exposed TOR-LM films. Optical transparency at 500 nm was measured on the CP films. The control sample exhibited a transparency of ~84% whereas the flight specimen was <1%. The sample was visibly frosted or opaque thus the low transparency was due to the scattering of light by the eroded film surface. Solar absorptivity ( $\alpha$ ) and thermal emissivity ( $\epsilon$ ) data was collected on CP films and TOR-LM films (Table 1). Solar absorptivity increased significantly due to the AO exposure. The increase in  $\alpha$  for the CP film was the same for the RAM facing side as well as the backside of the film. The polymer surface of the TOR-LM film exhibited a larger increase in  $\epsilon$  than the

colorless polyimide film. The exposed backside of the TOR-LM film, which had a VDA surface, did not exhibit any changes in  $\alpha$  or  $\varepsilon$ .

*Table 1. Solar Absorptivity/Thermal Emissivity*

Sample	$\alpha$	$\varepsilon$	$\alpha/\varepsilon$
CP control	0.07	0.67	0.11
CP exposed backside	0.23	0.71	0.32
CP RAM facing side	0.23	0.76	0.30
TOR-LM control (polymer surface)	0.31	0.71	0.44
TOR-LM control (VDA surface)	0.08	0.04	2.0
TOR-LM exposed backside (VDA surface)	0.08	0.04	2.0
TOR-LM RAM facing side (polymer surface)	0.50	0.85	0.59

As a means to investigate changes in surface chemistry, XPS was performed on all samples and on both sides of each film. The typical analysis depth was 2 to 5 nm, and a particular element (except hydrogen) can be measured down to 0.1% atomic fraction. By summing the area under the photoelectron peaks corresponding to different elements, the concentrations of those elements were determined (Tables 2-4).

*Table 2. XPS Analysis Results for TOR Thread*

Photoelectron	Control, Atomic Conc. %	Exposed, Atomic Conc. %
O 1s	19.3	26.7
N 1s	11.9	20.4
C 1s	67.8	51.3
P 2p	1.0	1.5

*Table 3. XPS Analysis Results for the CP film*

Photoelectron	Control, Atomic Conc. %	RAM Exposed, Atomic Conc. %	Backside Exposed, Atomic Conc. %
O 1s	16.3	46.5	36.4
N 1s	3.20	3.40	4.10
C 1s	78.9	38.1	51.3
P 2p	1.60	12.0	8.20

*Table 4. XPS Analysis Results for TOR-LM*

Photoelectron	Control, Atomic Conc. %	Exposed, Atomic Conc. %
O 1s	11.5	44.1
N 1s	2.1	4.7
C 1s	83.6	41.4
P 2p	2.7	10.0

To summarize the results from the XPS analyses, for each sample there is a noticeable increase in the oxygen and phosphorus concentration after exposure. The

high resolution O 1s signal from the samples could be fit with two peaks corresponding to two different bonding situations. The O 1s sub-peak at 530 eV is reduced while the sub-peak at 534 eV increases indicating that the oxygen has become more inorganic. After exposure the amount of phosphorus at the surface has increased. This is most likely in the form of an oxide (phosphate) since the binding energy of the P 2p<sub>3/2</sub> peak shifts from 132 eV to 135 eV. The amount of carbon is reduced presumably due to material loss via reaction with AO. In the case of CP, the changes in surface chemistry follow the same trend as those on the RAM facing side indicating that AO had access to the backside of the film. Changes in surface chemistry are due to reaction of polymeric material with AO and are consistent with those observed on other ground-based and short term flight exposure experiments.

AFM analyses were performed on the samples to investigate changes in surface topography. All samples showed an increase in surface roughness upon exposure both on the exposed backside and the RAM facing side (Table 5). Samples were also examined on the exposed side in the area that was protected by the metal mounting bars. Both film samples showed a significant increase in surface roughness on the RAM facing side when compared to the control sample. The exposed backside of the colorless polyimide film showed an increase in roughness compared to both the control and the exposed backside of TOR-LM. This is consistent with the XPS results showing that the exposed backside of the colorless polyimide film did experience exposure to AO. The exposed backside of the TOR-LM did not exhibit as much erosion (due to the VDA surface) but still had an increase in roughness compared to the control.

*Table 5. AFM analysis of surface roughness*

Sample	Average R <sub>a</sub> (nm)	Standard Deviation of R <sub>a</sub> (nm)	Average R <sub>q</sub> (nm)	Standard Deviation of R <sub>q</sub> (nm)
CP control	0.466	0.024	0.733	0.075
CP exposed backside	8.443	7.486	12.01	9.842
CP RAM facing side	419.1	371.7	517.1	452.1
CP RAM facing side*	80.21	80.66	99.17	95.40
TOR-LM exposed backside	1.757	0.704	2.364	1.435
TOR-LM exposed RAM facing side	427.4	206.0	525.2	245.0
TOR-LM exposed RAM facing side*	326.8	172.3	408.1	209.5

\*Under metal bar used to hold down the film sample

The exposed RAM facing surface of TOR-LM film showed what appeared to be platelet formations that served as etch stops in the material (Figure 4). Even though the RAM facing surface was significantly roughened, the platelets seemed to slow the etching where they formed. It is important to note that the average surface roughness and the relative standard deviation of the roughness both increased. This indicates that the sample did not roughen in a homogeneous fashion, consistent with the theory that the sample forms platelets that are comprised of a phosphate material that act as an etch stop.

The exposed thread sample (TOR) showed a decrease in overall diameter, an increase in surface roughness, and separation of the weave but the data cannot be

quantified due to the uneven surface features of the thread. Qualitatively, the thread sample was not noticeably degraded and could not be readily broken by hand.

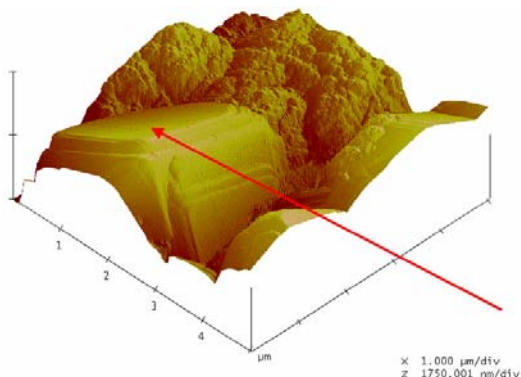


Figure 4. AFM image of the TOR-LM exposed RAM facing surface showing platelet formation (denoted by arrow). X and Y axis units are in  $\mu\text{m}$ .

**4. SUMMARY** Aromatic polymers containing PPO groups were exposed to LEO for ~4 years. The polymers survived intact despite high AO fluence whereas other polymers such as Kapton<sup>®</sup> and metallized polyimides were completely eroded. The polymer films appeared frosted and AO erosion significantly affected optical transparency as well as solar absorptivity and thermal emissivity of the film samples. The changes in surface chemistry as determined by XPS were consistent with the formation of a phosphate surface layer. Changes in surface topography consistent with AO erosion were evident from AFM analysis. The effects of LEO exposure on polymers containing PPO groups are consistent with those previously reported from shorter space flight exposure experiments. Due to the property changes exhibited by the films, the materials are perhaps more suitable for applications in LEO in the form of stitching thread, woven fabric, softgoods, or tethers.

**5. ACKNOWLEDGEMENTS** The authors would like to acknowledge Drs. Brian Holloway and Randy Collette from the Applied Science Department at the College of William and Mary for performing the XPS analyses.

## 6. REFERENCES

1. C.D. Smith, H. Grubbs, H.F. Webster, A. Gungor, J.P. Wightman and J.E. McGrath, High Performance Polymers, **3**(4), 211 (1991).
2. J.G. Smith, Jr., J.W. Connell and P.M. Hergenrother, Polymer, **35**(13), 2834 (1994).
3. J.W. Connell, J.G. Smith, Jr. and P.M. Hergenrother, Polymer, **36**(1), 5 (1995).
4. J.W. Connell, J.G. Smith, Jr. and J.L. Hedrick, Polymer, **36**(1), 13 (1995).
5. J.W. Connell, J.G. Smith, Jr., C.G. Kalil and E.J. Siochi, Polymers for Advanced Technologies, **9**(1), 11 (1998).
6. P. Schuler, R. Haghghat and H. Mojazza, High Performance Polymers, **11**(1), 113 (1999).
7. J.M. Zwiener, R.R. Kamenetzky, J.A. Vaughn, M.M. Finckenor and P. Peters, MIR-ISSA Risk Mitigation Flight Experiment RME One-Year Final Report, [http://setas-www.larc.nasa.gov/meep/1-year/posa\\_I/posa1\\_1\\_year.html](http://setas-www.larc.nasa.gov/meep/1-year/posa_I/posa1_1_year.html)
8. J.W. Connell, High Performance Polymers, **12**(1), 43 (2000).

9. P. Schuler, H. Mojazza and R. Haghghat, High Performance Polymers, 12(1), 113 (2000).
10. L.L. Fewell, J. App. Polym. Sci., 41, 391 (1990).
11. L.L. Fewell and L. Finney, Polymer, 32, 393 (1991).
12. W.S. Slemph, B. Santos-Mason, G.F. Sykes, Jr. and W.G. Witle, Jr., AO Effect Measurements for Shuttle Missions STS-8 and 41-G, 1(5), 1 (1985).
13. L.J. Leger, J.T. Visentine and B. Santos-Mason, SAMPE Q, 18(2), 48 (1987).
14. J.T. Visentine, L.J. Leger, J.F. Kuminecz and K.I. Spiker, AIAA 23<sup>rd</sup> Aerospace Conf Proc., AIAA-85-7021 (1985).
15. C.A. Arnold, J.D. Summers, Y.P. Chen, R.H. Bott, D.H. Chen and J.E. McGrath, Polymer, 30, 986 (1989).
16. C.A. Arnold, J.D. Summers, Y.P. Chen, T.H. Yoon, B.E. McGrath, D.H. Chen and J.E. McGrath, in 'Polyimides: Materials, Chemistry and Characterization' (Ed. C. Feger), Elsevier Science Publishers, Amsterdam, 1989 pp. 69-89.
17. C.A. Arnold, D.H. Chen, Y.P. Chen, R.O. Waldbauer, Jr., M.E. Rogers and J.E. McGrath, High Performance Polymers, 2(2), 83 (1990).
18. J.W. Connell, D.C. Working, T.L. St. Clair and P.M. Hergenrother, in 'Polyimides: Materials, Chemistry and Characterization' (Ed. C. Feger), Technomic, Lancaster, PA, 1993 pp. 152-164.
19. J.W. Connell, J.G. Smith, Jr. and P.M. Hergenrother, J. Fire Sci., 11(2), 137 (1993).
20. P.R. Young and W.S. Slemph, in "NASA CP 3162 Part 1", 1991 pp. 376-378.
21. J. Kulig, G. Jefferis and M. Litt, Polym. Mater. Sci. Eng., 61, 219 (1989).
22. A.E. Stiegman, D.E. Brinza, M.S. Anderson, T.K. Minton, G.E. Laue and R.H. Liang, Jet Propulsion Laboratory Publication 91-10, May (1991).
23. L.J. Leger, K.I. Spikes, J.F. Kuminecz, T.J. Ballentine and J.T. Visentine, "STS Flight 5, LEO Effects Experiment", AIAA-83-2631-CP (1983).
24. B.A. Banks, M.J. Mistich, S.K. Rutledge and H.K. Nahra, Proc. 18<sup>th</sup> IEEE Photovoltaic Specialists Conf., (1985).
25. K.A. Smith, "Evaluation of Oxygen Interactions with Materials, STS-8 AO Effects", AIAA-85-7021 (1985).
26. J.W. Gilman, D.S. Schlitzer and J.D. Lichtenhan, J. App. Polym. Sci., 60, 591 (1996).
27. A.L. Brunsvold, T.K. Minton, I. Gouzman, E. Grossman and R. Gonzalez, High Performance Polymers, 16(2), 303 (2004).
28. M.E. Wright, B.J. Petteys, A.J. Guenther, S. Fallis, G.R. Yandek, S.J. Tomczak, T.K. Minton and A.L. Brunsvold, Macromolecules, 39, 4710 (2006).
29. G. Pippin, Final Report Air Force Contract 02-S470-011-C1, July 2006.
30. K.A. Watson, F.L. Palmeri and J.W. Connell, Macromolecules, 35, 4968-4974 (2002).
31. ISO 4287-1997, ISO 4288-1996
32. J.W. Connell, J.G. Smith, Jr. and P.M. Hergenrother, in 'High Temperature Properties and Applications of Polymeric Materials', ACS Symposium Series 603 (M.R. Tant, J.W. Connell and H.L.N. McManus, Editors), American Chemical Society, Washington, DC, 1995 pp. 186-199.